

The University of Akron

IdeaExchange@UAkron

---

Williams Honors College, Honors Research  
Projects

The Dr. Gary B. and Pamela S. Williams Honors  
College

---

Spring 2023

## Intergranular and pitting corrosion mechanisms of sensitized aluminum alloy AA5083

Clayton Egleston  
cde30@uakron.edu

Follow this and additional works at: [https://ideaexchange.uakron.edu/honors\\_research\\_projects](https://ideaexchange.uakron.edu/honors_research_projects)



Part of the [Materials Chemistry Commons](#), and the [Other Materials Science and Engineering Commons](#)

Please take a moment to share how this work helps you [through this survey](#). Your feedback will be important as we plan further development of our repository.

---

### Recommended Citation

Egleston, Clayton, "Intergranular and pitting corrosion mechanisms of sensitized aluminum alloy AA5083" (2023). *Williams Honors College, Honors Research Projects*. 1693.

[https://ideaexchange.uakron.edu/honors\\_research\\_projects/1693](https://ideaexchange.uakron.edu/honors_research_projects/1693)

This Dissertation/Thesis is brought to you for free and open access by The Dr. Gary B. and Pamela S. Williams Honors College at IdeaExchange@UAkron, the institutional repository of The University of Akron in Akron, Ohio, USA. It has been accepted for inclusion in Williams Honors College, Honors Research Projects by an authorized administrator of IdeaExchange@UAkron. For more information, please contact [mjon@uakron.edu](mailto:mjon@uakron.edu), [uapress@uakron.edu](mailto:uapress@uakron.edu).



**Intergranular and pitting corrosion mechanisms  
of sensitized aluminum alloy AA5083**

Honors Project CHEE:497

Report submitted by:

**Clayton Egleston**

Honors Project Sponsor:

Dr. David M. Bastidas

Date: 12 April 2023

## Executive Summary

Over the past decade, the aluminum industry has invested more than \$7 billion in U.S. manufacturing to support the growing demand in key markets—aluminum has high demand because it is generally lightweight and corrosion resistant. Aluminum 5XXX alloys are widely used due to being lightweight, non-heat treatable, and commonly used in marine applications. The AA5083 is an aluminum-magnesium (Al-Mg) alloy, which is valued for its economic production, weldability, and corrosion resistance. The objective of this project is to examine the mechanisms of intergranular corrosion (IGC) and pitting corrosion of sensitized AA5083. In this regard, different characterization techniques were used, including optical analysis of microstructure, cyclic potentiodynamic polarization with Tafel fitting, electrochemical impedance spectroscopy with electrical equivalent circuit (EEC) fitting, and potentiostatic current transient monitoring. When exposed to elevated temperatures (50–200 °C) during working life of AA5083, the transition from IGC to pitting corrosion occurs when the grain boundaries become saturated with the  $\beta$ -phase ( $\text{Mg}_2\text{Al}_3$ ), making it sensitized.

In this experiment, samples of AA5083 were aged at 150 °C for 0, 7, 14, 22, and 28 days for varying degrees of sensitization. ASTM G110-92 was followed for the degree of sensitization (DoS) test with each sample being etched in 0.4M acidified ammonium persulfate prior to..... DoS increased as thermal treatment time increased with a moderate logarithmic trend—DoS increases less rapidly at longer sensitization times.

For electrochemical testing of the AA5083 samples a Gamry Series 600 potentiostat was used. The setup for each test consisted of three electrodes: an AA5083 sample as the working electrode, graphite as the counter electrode, and a saturated KCl calomel (SCE) as the reference

electrode. Each sample was mounted to achieve a flat working area of about  $1 \text{ cm}^2$  then immersed in a 3.5% NaCl solution at room temperature ( $\sim 25 \text{ }^\circ\text{C}$ ) for testing.

Cyclic potentiodynamic polarization (CPP) is a common non-destructive test for evaluating susceptibility to repassivation and calculating pitting corrosion rates. During CPP testing, a wide range of voltage is applied on the test electrode (AA5083) starting at the open circuit potential, where the overall change in current can be observed, then the voltage returns to the starting point. It was found that the corrosion rate,  $E_{\text{corr}}$ , decreases from  $-822 \text{ mV}_{\text{SCE}}$  at no thermal treatment to a value of  $-942 \text{ mV}_{\text{SCE}}$  at 28 days of exposure to  $150 \text{ }^\circ\text{C}$  as the sensitization time increased (values became more negative). The corrosion current,  $i_{\text{corr}}$ , increased from  $0.193 \times 10^{-6} \text{ A/cm}^2$  at 0 days of thermal treatment to a maximum of  $1.470 \times 10^{-6} \text{ A/cm}^2$  as sensitization time increased.

Electrochemical impedance spectroscopy (EIS) is another non-destructive test for characterizing mechanisms of corrosion. The test measures an alternating current to an applied alternating potential over a range of frequencies, typically from  $10^{-1} - 10^5 \text{ Hz}$ . From the measurement, the polarization resistance and double layer capacitance can be obtained. The oxide film admittance and double layer admittance increase as sensitization increases.

The key finding in this experiment was the logarithmically increasing degree of sensitization trend. When exposed to a saline environment at elevated temperatures, AA5083 becomes more susceptible to pitting corrosion when the grain boundaries become saturated with the  $\beta$ -phase ( $\text{Mg}_2\text{Al}_3$ ).

## **Abstract**

The motivation and objectives of this project is to examine the mechanisms of intergranular corrosion (IGC) and pitting corrosion of sensitized AA5083. In this regard, different characterization techniques were used, including optical analysis of microstructure, cyclic potentiodynamic polarization with Tafel fitting, electrochemical impedance spectroscopy with electrical equivalent circuit (EEC) fitting, and potentiostatic current transient monitoring. The transition from IGC to pitting corrosion occurs when the grain boundaries become saturated with the  $\beta$ -phase ( $Mg_2Al_3$ ). It was found that AA5083 becomes more vulnerable to pitting corrosion as the degree of sensitization increases.

## **1. Introduction**

Over the past decade, the aluminum industry has invested more than \$7 billion in U.S. manufacturing to support the growing demand in key markets—aluminum has high demand because it is generally lightweight and corrosion resistant [1]. The global cost of corrosion is estimated to be 2.5 trillion USD which is a significant portion of the global GDP (2015); however, an estimated 15–35% of the cost could be achieved with modern corrosion control practices [2]. Corrosion is a destructive reaction over time of a material with the surrounding environment [3]. Aluminum 5XXX alloys are widely used due to being lightweight, non-heat treatable, and commonly used in marine applications. The AA5083 is an aluminum-magnesium (Al-Mg) alloy, which is valued for its economic production, weldability, and corrosion resistance [4]. The supersaturated magnesium content (4.0–4.9 wt%) in the solid solution of AA5083 provides improved mechanical properties and strength, at the expense of susceptibility to intergranular (IGC) corrosion when exposed to high temperatures [5]. Because AA5083 is used in marine

applications, the saline environment can also accelerate the corrosion of the relatively corrosion resistant alloy.

## 2. Background

When exposed to elevated temperatures (50–200 °C) during working life of AA5083, IGC and pitting due to Al-Mg intermetallics in the alloy form the  $\beta$ -phase ( $Mg_2Al_3$ ) in the grain boundaries, making it sensitized [6]. The degree of sensitization (DoS) test for AA5XXX alloys is typically performed on the basis of the nitric acid mass lost test (NAML), according to ASTM G67-18 [16]. One alternative DoS test is ASTM G110-92 which utilizes a sodium chloride and hydrogen peroxide solution [8]. Both DoS tests measure the mass loss per unit area over a period of 24 hours. Sensitized samples are vulnerable to intergranular corrosion and pitting because the  $\beta$ -phase precipitates at the grain boundaries [9].

Cyclic potentiodynamic polarization (CPP) is a common non-destructive test for evaluating susceptibility to repassivation and calculating pitting corrosion rates. During CPP testing, a wide range of voltage is applied on the test electrode (AA5083) starting at the open circuit potential, where the overall change in current can be observed, then the voltage returns to the starting point [10]. The CPP is advantageous due to its quick and easily interpretable results [11]. A common method of analyzing CPP curves is a Tafel fit which gives the corrosion rate of potentiodynamic data [12]. Electrochemical impedance spectroscopy (EIS) is another non-destructive test for characterizing mechanisms of corrosion [13]. The test measures an alternating current to an applied alternating potential over a range of frequencies, typically from  $10^{-1}$  –  $10^5$  Hz. From the measurement, the polarization resistance and double layer capacitance can be obtained—the most common way to analyze EIS tests is through the use of the common electrical equivalent circuit

(EEC) [14]. Current transient testing can be used to calculate the total charge for specimens to compare to DoS results to identify trends [15].

### 3. Experimental

**Table 1** contains the elemental composition of AA5083 as received. The samples were cut to  $10 \times 10 \times 3$  mm then aged in a furnace at  $150\text{ }^{\circ}\text{C}$  for sensitization. The samples were taken out at exposure times of 7, 14, 22, and 28 days then cooled in air.

**Table 1.** Elemental composition of AA5083 according to element wt%.

Element	Mg	Si	Fe	Cu	Mn	Zn	Cr	Ti	Al
wt%	4.4	0.08	0.19	0.026	0.56	0.004	0.077	0.015	Balance

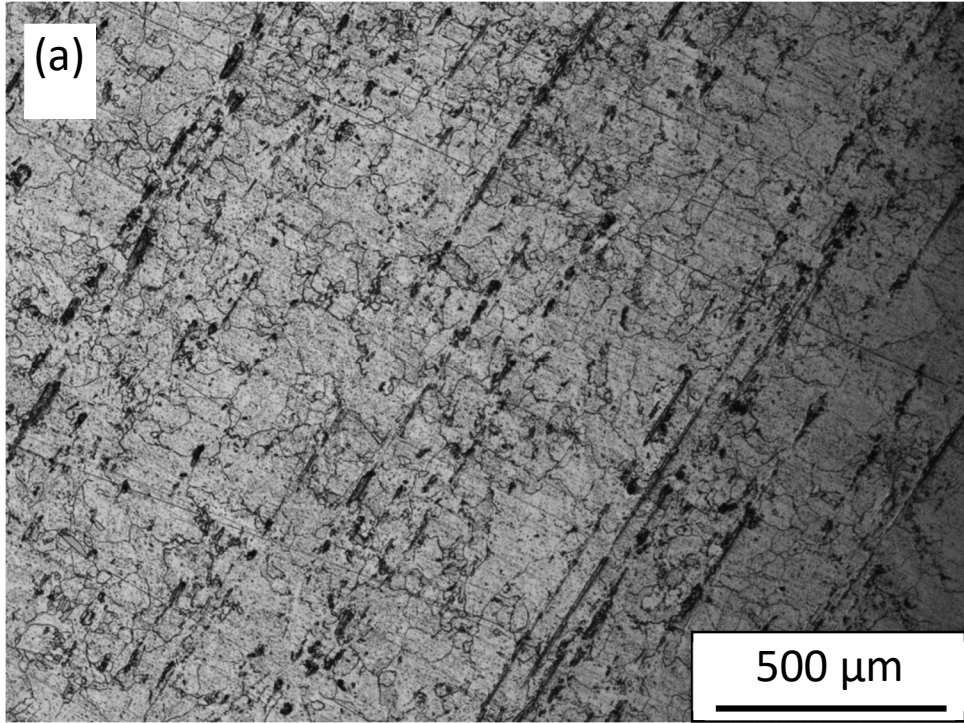
The AA5083 samples were ground with SiC paper on each face to 1200 grit and washed with water then air dried. ASTM G110-92 was followed for the DoS test. Each sample was etched in 0.4M acidified ammonium persulfate for 1 min then dried and weighed. The samples were immersed in a solution of 57 grams sodium chloride with 10 mL hydrogen peroxide diluted to 1 L with deionized (DI) water per ASTM G110-92. After 24 hours, the samples were removed from solution then washed and dried prior to recording the weight once again. Each sample was repolished and etched in the same 0.4 M acidified ammonium persulfate solution then rinsed with ethanol and dried. An optical microscope was used for visual analysis of the grain structure of the sensitized samples.

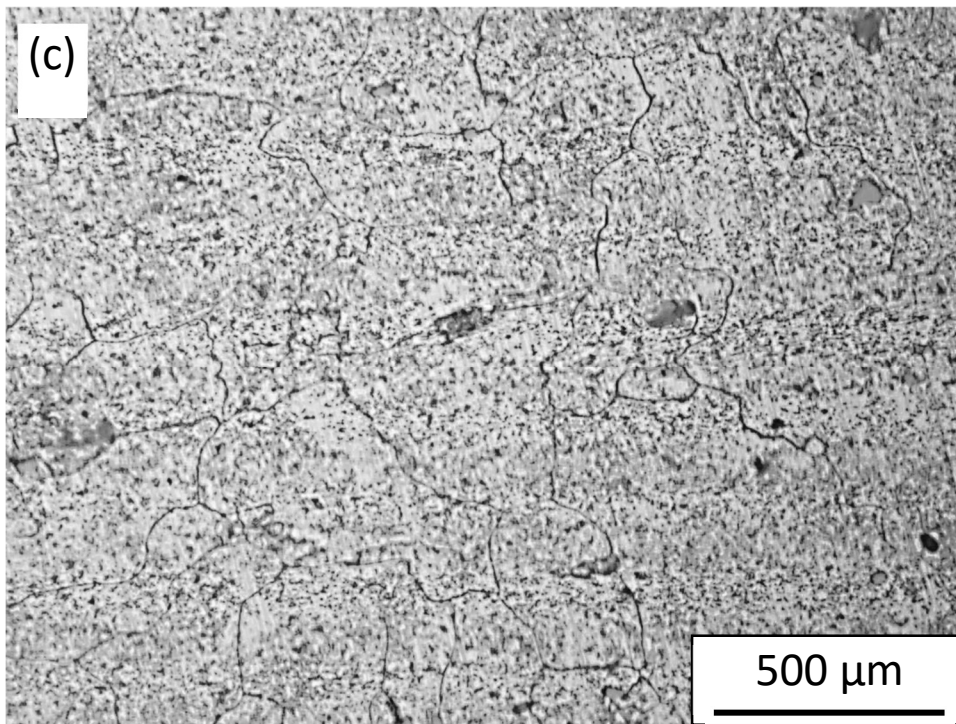
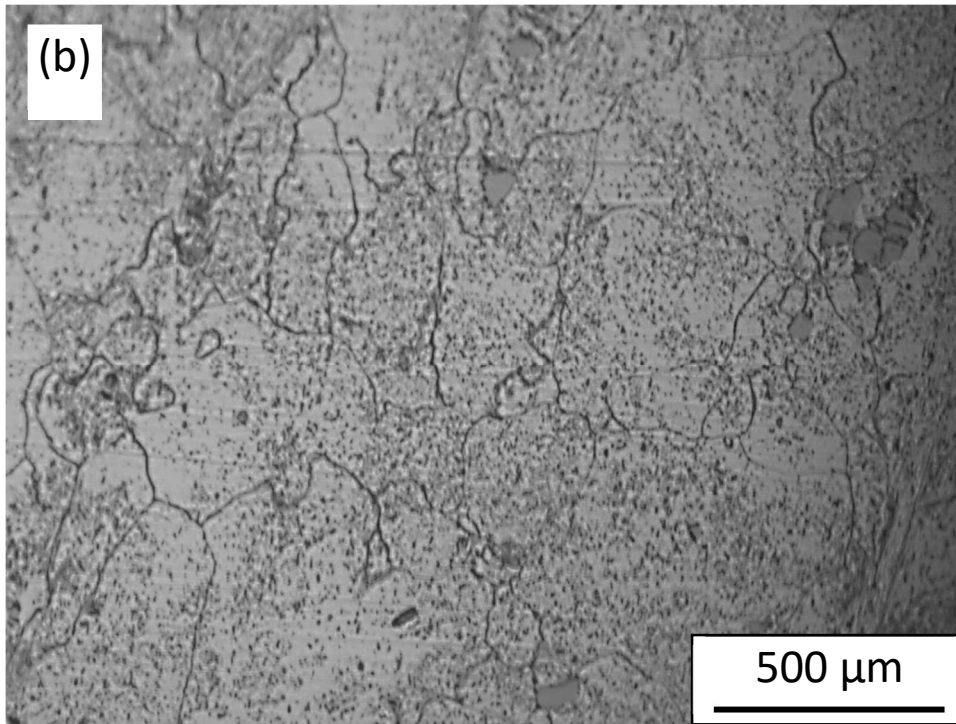
For electrochemical testing of the AA5083 samples a Gamry Series 600 potentiostat (Gamry Instruments, Warminster, PA, USA) was used. The setup for each test consisted of three

electrodes: an AA5083 sample as the working electrode, graphite as the counter electrode, and a saturated KCl calomel (SCE) as the reference electrode. Each sample was mounted to achieve a flat working area of about  $1 \text{ cm}^2$  then immersed in a 3.5% NaCl solution at room temperature ( $\sim 25^\circ\text{C}$ ) for testing. The electrochemical tests conducted were open circuit potential (OCP), EIS, CPP, and current transient. The OCP was measured for an hour to get a stable potential value for both the EIS and CPP. EIS was conducted with an AC voltage of 10 mV rms over a range of  $10^{-2} - 10^5$  Hz using 10 points per decade. An EEC model was constructed to fit the EIS curve to obtain admittance and resistance values for the oxide film and double layer. CPP testing was conducted at an initial value of  $-200 \text{ mV}_{\text{OCP}}$  to a final value of  $+200 \text{ mV}_{\text{OCP}}$  with a forward and reverse scanning rate of  $1.66 \text{ mV/s}$ . The values for  $E_{\text{corr}}$  and  $i_{\text{corr}}$  were obtained from the Tafel fit. Current transient tests were conducted with a potential value of  $-710 \text{ mV}_{\text{SCE}}$  for 3600 seconds at a sample period of 1 second.

#### 4. Results and Discussion

The images for microstructure analysis from the optical microscope for each sample after the acidified ammonium persulfate etching are shown in **Figure 1**. For **Figure 1a**, the 0 day sample (no thermal treatment) grain boundary outlines can be partially seen by the thin dark lines. As observed by the dark outlines in **Figure 1b**, more dissolution of the  $\beta$ -phase at the grain boundaries as sensitization time increases. In **Figures 1c-e**, the dark lines remain well-defined with dark specs in the intragranular regions becoming more prominent. The increasing amount of dark intragranular spots of the  $\beta$ -phase indicate a transition away from IGC due to saturation at the grain boundaries, leading to pitting corrosion.





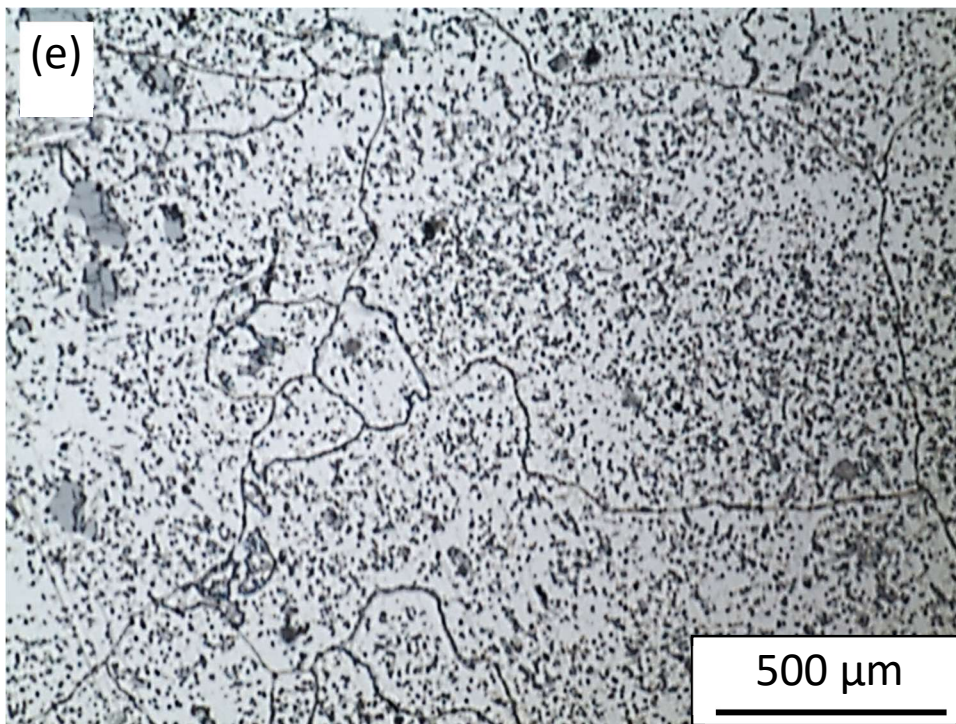
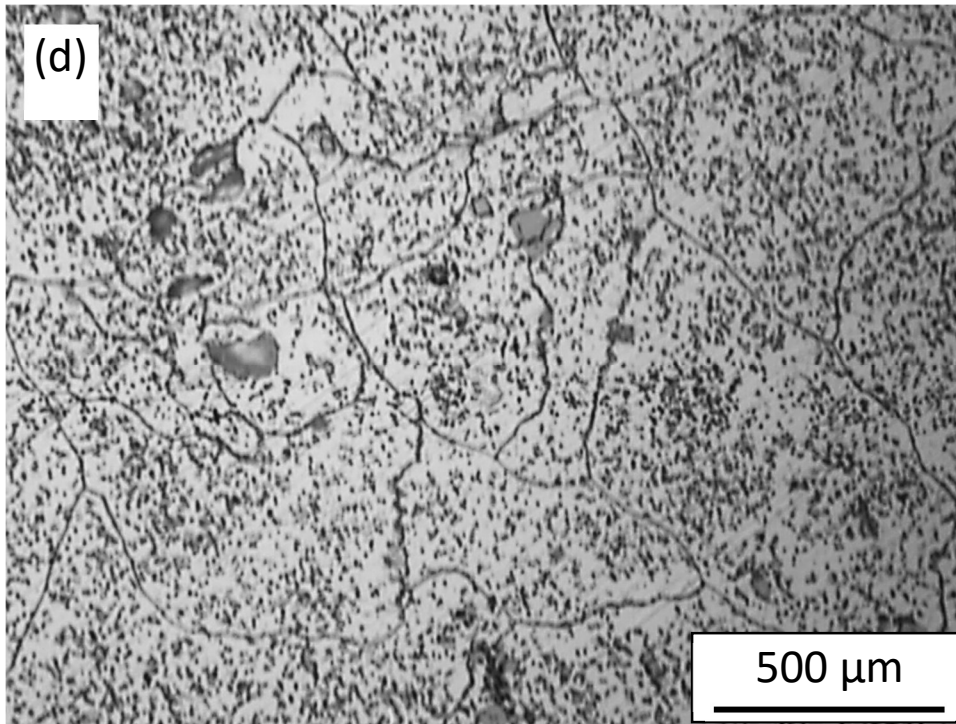


**Figure 1.** Optical microscope images of AA5083 samples etched with 0.4 M ammonium persulfate sensitized at 150 °C for (a) 0 days, (b) 7 days, (c) 14 days, (d) 22 days, and (e) 28 days.

Degree of sensitization increased from about 0.1 mg/cm<sup>2</sup> with no thermal treatment to 0.559 mg/cm<sup>2</sup> with 28 days of exposure at 150 °C. DoS trends start to level off after about 14 days as shown by **Figure 2** with the values shown in **Table 2**. The DoS values are low overall compared to that of the ASTM G67-18 nitric acid mass loss test (NAMLT) because ASTM G110-92 uses a much weaker solution [16]. The CPP testing results can be seen in **Figure 3** and **Table 2**. The Tafel fits showed a decreasing corrosion rate,  $E_{\text{corr}}$ , from -822 mV<sub>SCE</sub> at no thermal treatment to a value of -942 mV<sub>SCE</sub> at 28 days of exposure to 150 °C as the sensitization time increased (values became more negative). The corrosion current,  $i_{\text{corr}}$ , increased from  $0.193 \times 10^{-6}$  A/cm<sup>2</sup> at 0 days of thermal treatment to a maximum of  $1.470 \times 10^{-6}$  A/cm<sup>2</sup> as sensitization time increased. The corrosion current increased at a rate of about  $0.350 \times 10^{-6}$  A/cm<sup>2</sup> every 7 days of exposure at 150 °C. The corrosion current value was obtained from the intersection of the slopes in the Tafel fitting. The increasing corrosion rate and current indicate a more active surface as exposure time increases. The more active surface correlates with higher degree of sensitization leading to increased susceptibility to corrosion.

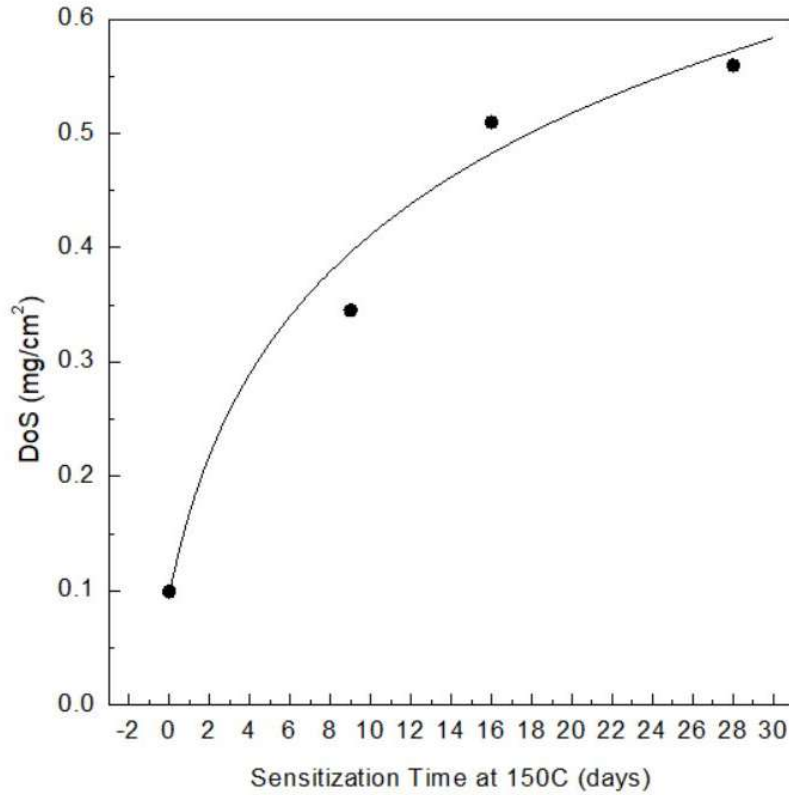


**Figure 2.** The degree of sensitization values for AA5083 sensitized at 150 °C after immersion in hydrogen peroxide + NaCl solution according to ASTM G110-92.

**Table 2.** The degree of sensitization,  $E_{\text{corr}}$ , and  $i_{\text{corr}}$  values for samples sensitized at 150 °C for 0, 7, 14, and 28 days. The DoS values were obtained from the G110-92 mass loss test while the  $E_{\text{corr}}$  and  $i_{\text{corr}}$  values were obtained from Tafel fitting.

Sensitization Time (days)	DoS (mg/cm <sup>2</sup> )	$E_{\text{corr}}$ (mV <sub>SCE</sub> )	$i_{\text{corr}}$ (mA/cm <sup>2</sup> )
0	0.099	-822	193
7	0.345	-838	566
14	0.510	-873	833
28	0.559	-942	1470

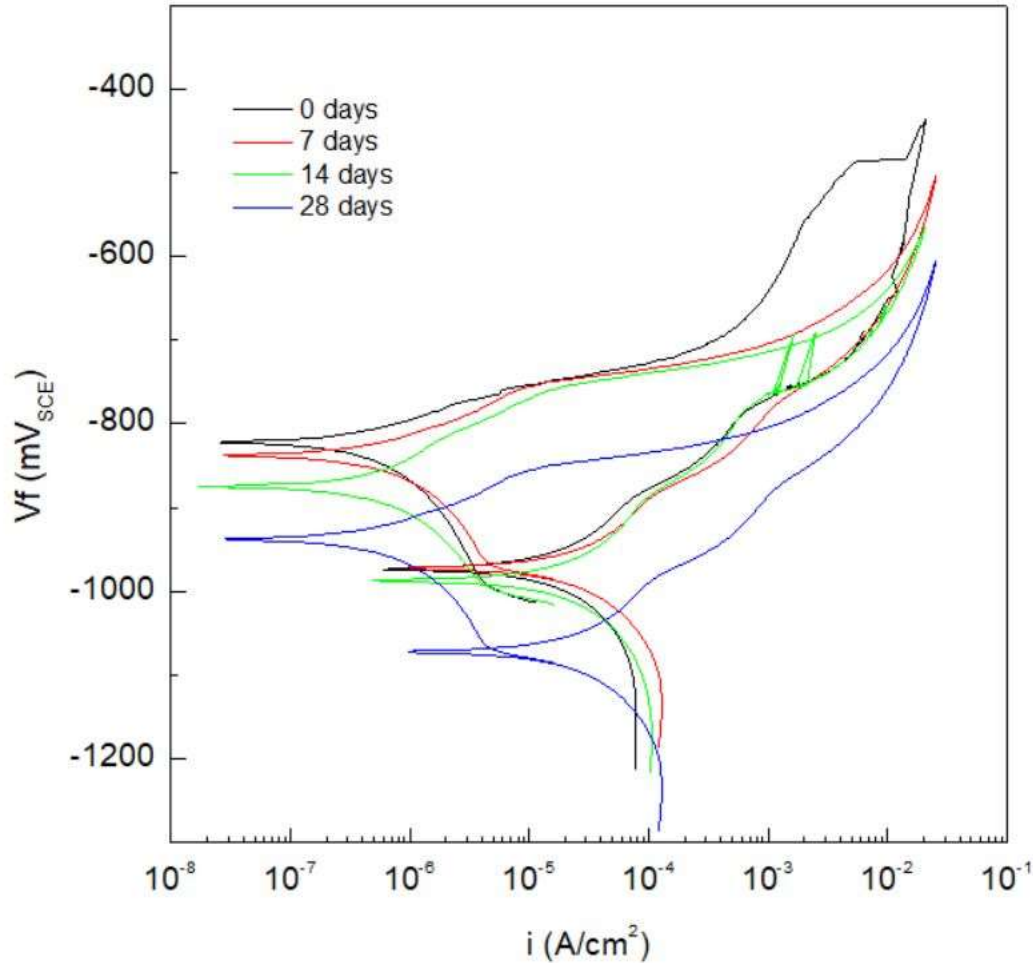


**Figure 3.** The cyclic potentiodynamic polarization (CPP) curves in 3.5% NaCl solution for AA5083 samples sensitized at 150 °C for 0 days, 7 days, 14 days, and 28 days. The Tafel fitting values are contained in **Table 2**.

The Bode plots are shown in **Figure 4** for sensitization time at 150 °C of 0 days, 14 days, and 28 days. The electrical equivalent circuit (EEC) is shown in **Figure 5** which was used for the fitting summarized in **Table 3**. The  $R_e$  is the resistance of the 3.5% NaCl test solution in each case which was about  $9 \Omega \text{ cm}^2$ . The  $R_f$  and  $R_{ct}$  are the resistances of the oxide film and charge transfer, respectively. The resistance values came out very inconsistent so there are no clear trends in the

data. The inconsistency is likely due to human error in setting up the tests, but the goodness of values is in a consistently low range (between  $10^{-4}$  and  $10^{-5}$ ). Despite the lack of trends in  $R_f$  and  $R_{ct}$ , there is little fluctuation in the values. In electrical circuits, the admittance is defined as the reciprocal of the capacitance. The admittance of the oxide film and double layer are  $Y_f$  and  $Y_{dl}$ , respectively. The  $Y_f$  increased from  $1.89 \times 10^{-5} \text{ S cm}^{-2} n_f$  at 0 days thermal treatment to a maximum of  $3.77 \times 10^{-5} \text{ S cm}^{-2} n_f$ , the  $Y_{dl}$  increased from  $2.76 \text{ S cm}^{-2} n_{dl}$  at 0 days to  $3.90 \times 10^{-5} \text{ cm}^{-2} n_{dl}$  at 28 days of sensitization at  $150 \text{ }^\circ\text{C}$ . The  $n_f$  and  $n_{dl}$  parameters are the exponential fitting coefficients for the oxide film and double layers, respectively. Both fitting values ranged from about 0.8 to 0.9 for every sample.

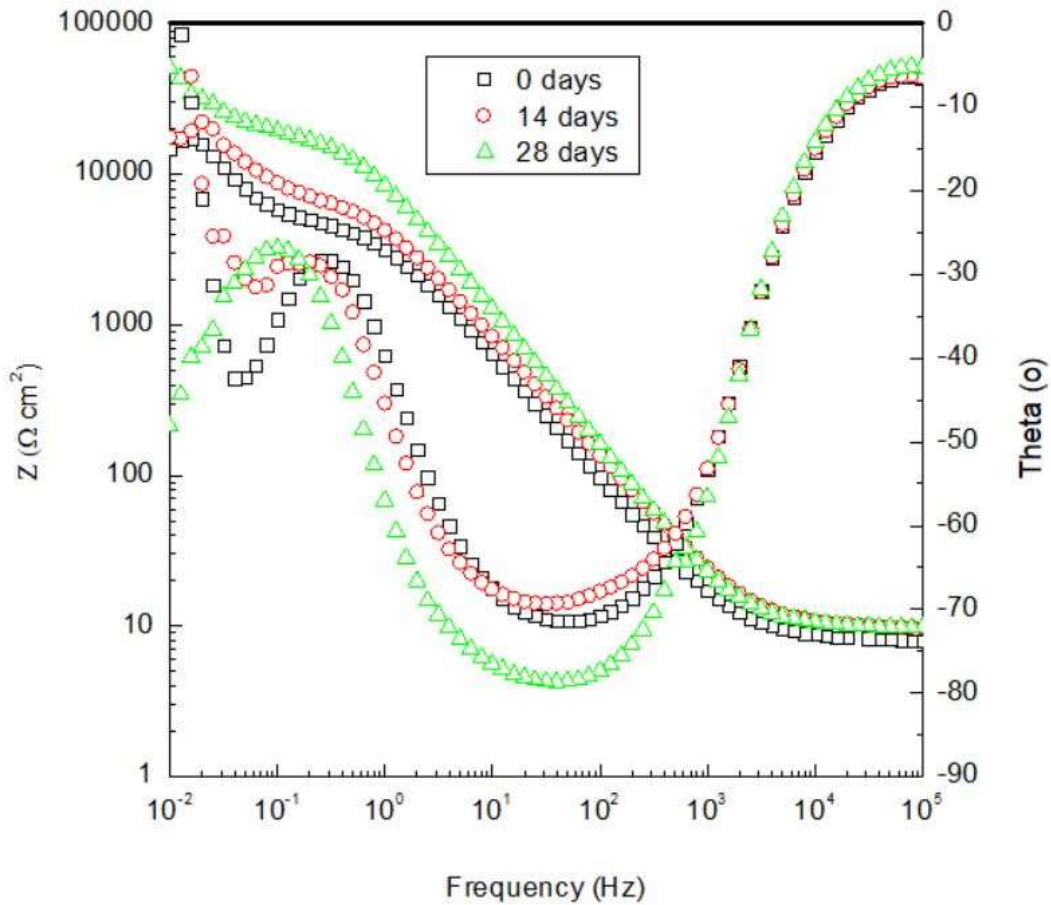


**Figure 4.** The Bode plots for AA5083 samples sensitized at 150 °C for 0 days, 14 days, and 28 days tested in 3.5% NaCl solution.

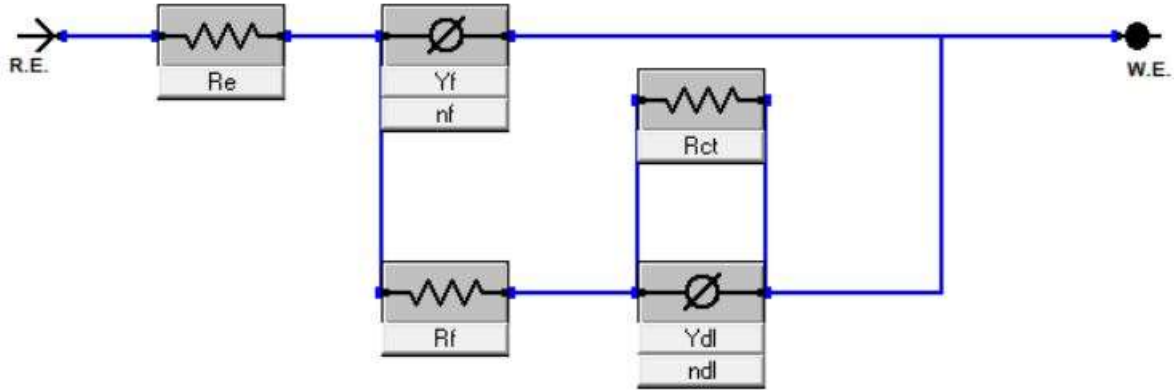


**Figure 5.** The impedance model of the electrical equivalent circuit (EEC) used to fit the AA5083 in 3.5% NaCl model.

**Table 3.** The values for  $R_e$ ,  $R_f$ ,  $R_{ct}$ ,  $Y_f$ ,  $Y_{dl}$ ,  $n_{dl}$ ,  $n_f$ , and goodness of fit from the EIS fitting based on the simple EEC model in **Figure 5**.

Sensitization Time (days)	$R_e$ ( $\Omega \text{ cm}^2$ )	$R_f$ ( $\Omega \text{ cm}^2$ )	$Y_f$ ( $\text{S cm}^{-2} n_f$ )	$n_f$	$R_{ct}$ ( $\Omega \text{ cm}^2$ )	$Y_{dl}$ ( $\text{S cm}^{-2} n_{dl}$ )	$n_{dl}$	$\chi^2$
0	10.05	2120	$1.89 \times 10^{-5}$	0.90	13500	$2.76 \times 10^{-5}$	0.88	$4.17 \times 10^{-4}$
7	9.4	1630	$2.04 \times 10^{-5}$	0.79	14100	$3.28 \times 10^{-5}$	0.85	$3.46 \times 10^{-4}$
14	9.6	8350	$2.79 \times 10^{-5}$	0.82	14400	$3.44 \times 10^{-5}$	0.91	$5.04 \times 10^{-4}$
28	8.5	5420	$3.77 \times 10^{-5}$	0.85	13800	$3.90 \times 10^{-5}$	0.89	$1.92 \times 10^{-4}$

The potentiostatic current transient curves in the 3.5% NaCl solution are shown in **Figure 6**. The peak current density increases as the sensitization time at 150 °C increases. The 0- and 7-day samples showed a gradual level off on the graphs of current density while the 14, 22, and 28

days have a sharp decrease right after the peak before leveling off. The 28 day sample had the highest peak current density of about  $7 \times 10^{-2} \text{ A/cm}^2$  while the 0 day sample had the lowest peak current density of about  $2 \times 10^{-2} \text{ A/cm}^2$ . When integrating the area under the curve with respect to time, a total charge value can be achieved. After integration, 28 days would have the largest total charge with the total charge decreasing as the sensitization time decreased. The relationship between total charge and sensitization time follows the same trend identified in the mass loss test.

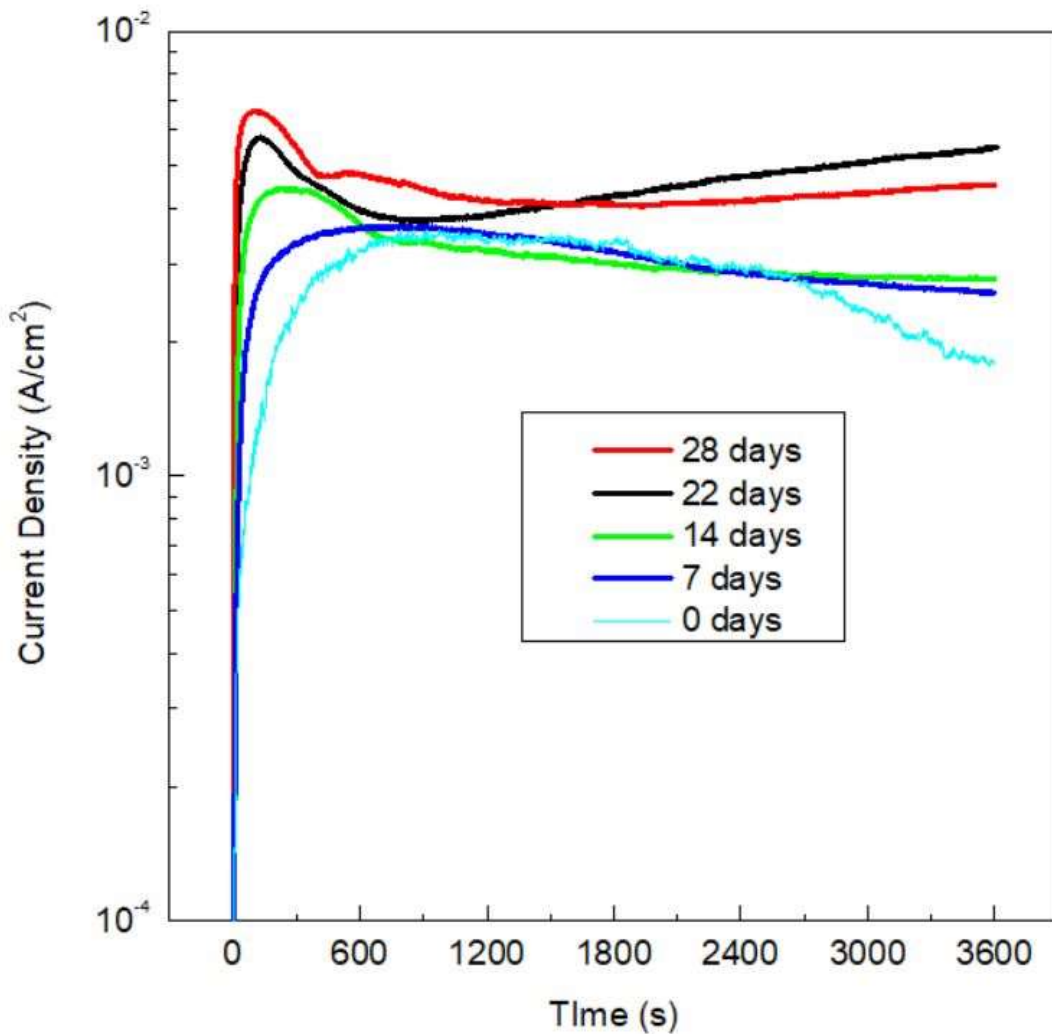


**Figure 6.** The current transient curves in 3.5% NaCl solution for AA5083 samples aged at 150 °C for 0 days, 7 days, 14 days, 22 days, and 28 days.

## Conclusions

The objective of the experiment was to examine the mechanisms of intergranular corrosion (IGC) and pitting corrosion of AA5083 using optical analysis of microstructure, cyclic potentiodynamic polarization with Tafel fitting, electrochemical impedance spectroscopy with electrical equivalent circuit (EEC) fitting, and potentiostatic current transient monitoring. It was found that degree of sensitization followed a logarithmically increasing trend as exposure time to 150 °C increased. The trend is explained by the grain boundaries being saturated with the  $\beta$ -phase as sensitization increases leading to an increased vulnerability to pitting corrosion.

## References

1. "U.S. Aluminum Drives Modern Manufacturing." The Aluminum Association. The Aluminum Association, March 16, 2023. <https://www.aluminum.org/>.
2. "Economic Impact." [impact.nace.org](http://impact.nace.org). NACE International, 2015. <http://impact.nace.org/economic-impact.aspx>.
3. "What Is Corrosion." AMPP. AMPP. Accessed April 10, 2023. <https://www.ampp.org/technical-research/what-is-corrosion#:~:text=Corrosion%20Basics%2C%20An%20Introduction%20explains,electrochemical%20reaction%20with%20its%20environment>.
4. Chuanjun Huang *et al* 2017 *IOP Conf. Ser.: Mater. Sci. Eng.* **279** 012002
5. Sivam, S. P. S. S., Abburi Lakshman Kumar, K. Sathiya Moorthy, and Rajendra Kumar. "Investigation exploration outcome of heat treatment on corrosion resistance of AA 5083 in marine application." *International Journal of Chemical Sciences* 14, no. S2 (2016): 453-460.
6. Yi, Gaosong, Alexander T. Derrick, Yakun Zhu, and Michael L. Free. "A Collector Plate Mechanism-Based Classical Intergranular Precipitation Model for Al Alloys Sensitized at Different Temperatures." *Metallurgical and Materials Transactions A* 46, no. 11 (2015): 5393–5406. <https://doi.org/10.1007/s11661-015-3110-2>.
7. Goswami, Ramasis, and Ronald L. Holtz. "Transmission Electron Microscopic Investigations of Grain Boundary Beta Phase Precipitation in Al 5083 Aged at 373 K (100 °C)." *Metallurgical and Materials Transactions A* 44, no. 3 (2012): 1279–89. <https://doi.org/10.1007/s11661-012-1166-9>.
8. "Standard Practice for Evaluating Intergranular Corrosion Resistance of Heat Treatable Aluminum Alloys by Immersion in Sodium Chloride + Hydrogen Peroxide Solution." ASTM International - Standards Worldwide. ASTM International, 2015. <https://www.astm.org/g0110-92r15.html>.
9. Hodge, Andrea M. "Study of  $\beta$  Precipitation and Layer Structure Formation in AL 5083: The Role of Dispersoids and Grain Boundaries." *Journal of Alloys and Compounds* 703 (2017): 242–50. <https://doi.org/10.1016/j.jallcom.2017.01.360>.
10. Esmailzadeh, S., Aliofkhazraei, M. & Sarlak, H. Interpretation of Cyclic Potentiodynamic Polarization Test Results for Study of Corrosion Behavior of Metals: A Review. *Prot Met Phys Chem Surf* 54, 976–989 (2018). <https://doi.org/10.1134/S207020511805026X>
11. Munir, Selin, Matthew H. Pelletier, and William R. Walsh. "Potentiodynamic Corrosion Testing." *Journal of Visualized Experiments*, no. 115 (2016). <https://doi.org/10.3791/54351>.

12. “Potentiodynamic and Cyclic Polarization Scans.” Gamry Instruments | Market Leader in the Support of Electrochemical Research. Gamry Instruments, Inc., June 25, 2019. <https://www.gamry.com/application-notes/corrosion-coatings/potentiodynamic-cyclic-polarization/>.
13. Orozco-Cruz, Ricardo, Ricardo Galvan-Martinez, Enrique A. Martínez, and Imelda Fernandez-Gómez. “Electrochemical Impedance Spectroscopy (EIS) Applied to Study to Aluminum Alloys Degradation in Saline Solution.” *ECS Transactions* 29, no. 1 (2010): 73–80. <https://doi.org/10.1149/1.3532305>.
14. Torne, Karin Beaussant, and Dan Persson. “Electrochemical Impedance Spectroscopy (EIS) for Non-Destructive Determination of Corrosion Mechanisms.” RISE. RISE RESEARCH INSTITUTES OF SWEDEN. Accessed April 10, 2023. [https://www.ri.se/en/what-we-do/services/eis-for-determination-of-corrosion-mechanisms#:~:text=Electrochemical%20impedance%20spectroscopy%20\(EIS\)%20is,electrochemical%20processes%20such%20as%20corrosion](https://www.ri.se/en/what-we-do/services/eis-for-determination-of-corrosion-mechanisms#:~:text=Electrochemical%20impedance%20spectroscopy%20(EIS)%20is,electrochemical%20processes%20such%20as%20corrosion).
15. J. Ress, U. Martin, J. Bosch, R. K. Gupta, and D. M. Bastidas, Intergranular to intragranular pitting corrosion transition mechanism of sensitized AA5083 at 150 °C, *Metals* 10 (2020) 1082. <https://doi.org/10.3390/met10081082>
16. “Standard Test Method for Determining the Susceptibility to Intergranular Corrosion of 5xxx Series Aluminum Alloys by Mass Loss after Exposure to Nitric Acid (NAMLT Test).” ASTM International - Standards Worldwide. ASTM International, January 2019. <https://www.astm.org/g0067-18.html>.